

# Archeops, mapping the CMB sky from large to small angular scales

J.-Ch. Hamilton <sup>a b</sup>, on behalf of the Archeops Collaboration.

<sup>a</sup>Institut des Sciences Nucléaires, CNRS-IN2P3, Grenoble, France

<sup>b</sup>Physique Corpuculaire et Cosmologie, CNRS-IN2P3, Collège de France, Paris, France

Archeops is a balloon-borne experiment designed to measure the temperature fluctuations of the CMB on a large region of the sky ( $\simeq 30\%$ ) with a high angular resolution (10 arcminutes) and a high sensitivity ( $60\mu\text{K}$  per pixel). Archeops will perform a measurement of the CMB anisotropies power spectrum from large angular scales ( $\ell \simeq 30$ ) to small angular scales ( $\ell \simeq 800$ ). Archeops flew for the first time for a test flight in July 1999 from Sicily to Spain and the first scientific flight took place from Sweden to Russia in January 2001. The data analysis is on its way and I present here preliminary results, realistic simulations showing the expected accuracy on the measurement of the power spectrum and perspectives for the incoming flights (Winter 2001/2003).

## 1. Introduction

### 1.1. CMB physics

In the framework of Big-Bang theory, the Universe started with a hot and dense phase about 15 billion years ago and cooled down while expanding. The first neutral atoms formed when the temperature was about 13.6 eV (160000 K), but due to the large number of photons compared to baryons (ratio  $\simeq 10^9$ ), the Universe remained ionized until the temperature dropped below 0.3 eV (3000 K). At this moment, the mean free path of the photons increased drastically so that the photons that scattered at this time have not interacted with matter since then. This moment is known as *matter-radiation decoupling* or *recombination*. Those photons cooled down with the expansion of the Universe and are now observed at a temperature of 2.7 K. As the matter and radiation were at thermal equilibrium before decoupling, these photons have a pure blackbody spectrum and are homogeneously distributed on the celestial sphere. This radiation is known as the *Cosmic Microwave Background* (hereafter CMB).

The discovery of the CMB by Penzias and Wilson [1] and its interpretation in terms of a Big-Bang relic by Dicke and collaborators [2] was a major argument for the Big-Bang theory [3,4]. The CMB temperature was measured to be highly isotropic but tiny anisotropies were expected.

These temperature fluctuations reflect the density fluctuations on the last scattering surface. These are necessary to explain the presence of structures in the Universe such as galaxies and clusters. The CMB anisotropies were discovered by the COBE satellite with a *rms* amplitude of about  $30\mu\text{K}$  [5] at scales larger than 7 degrees. COBE also measured its spectrum with high precision [6,7] proving its pure blackbody nature.

The CMB anisotropy typical physical size in the last scattering surface can be theoretically predicted while its angular size as seen from here and now depends on the geometry of the Universe along the path of the photons. Hence, mapping the CMB anisotropies is a powerful cosmological test.

The two competing paradigms for the origin of structures in the Universe, namely inflation and topological defects, predict significantly different distributions for the former density fluctuations. These distributions propagate to us in a cosmological parameters dependent way to describe the temperature anisotropies that we expect on the sky<sup>1</sup>. It is therefore of deep interest to investigate their angular distribution and compare the measurements to cosmological models.

The temperature anisotropies on the sky are

---

<sup>1</sup>Freely available numerical codes, such as CMBFast [8], have been developed for this purpose.

commonly described via their spherical harmonics expansion,

$$\frac{\delta T}{T}(\theta, \phi) = \sum_{\ell=0}^{\infty} \sum_{m=-\ell}^{\ell} a_{\ell m} Y_{\ell m}(\theta, \phi), \quad (1)$$

where  $\ell$  is the multipole index, inversely proportional to the angular scale (1 degree roughly corresponds to  $\ell = 200$ ). The angular power spectrum of the temperature fluctuations of the CMB is defined as:

$$C_{\ell} = \frac{1}{2\ell+1} \sum_{m=-\ell}^{\ell} |a_{\ell m}|^2. \quad (2)$$

The evolution of the angular power spectrum of the CMB as a function of  $\ell$  can be splitted into three major regions (see Figure 1):

- On the low- $\ell$  part (large angular scales) no particular structure is expected as we are considering physical sizes on the last scattering surface larger than the horizon at the epoch of decoupling. No physical process is expected to have modified those fluctuations since the early Universe.
- Between  $\ell \simeq 30$  and  $\ell \simeq 1000$  (degree and sub-degree scales) we are considering structures that had time to collapse and experience acoustic oscillations between the matter-radiation equality and the matter-radiation decoupling. We therefore expect a series of acoustic peaks (the first one being located around  $\ell = 200$ , corresponding to the size of the horizon at the epoch of decoupling) in the case of inflationary-like early Universe models where the oscillations are in phase. In the case of isocurvature fluctuations (such as topological defects), the oscillations are not in phase and a large bump is expected, but no multiple peaks.
- In the large  $\ell$  part (arcminute scales and below), the power is expected to drop drastically due to the finite thickness of the last scattering surface and to the finite value of the mean free path of the photons before decoupling.

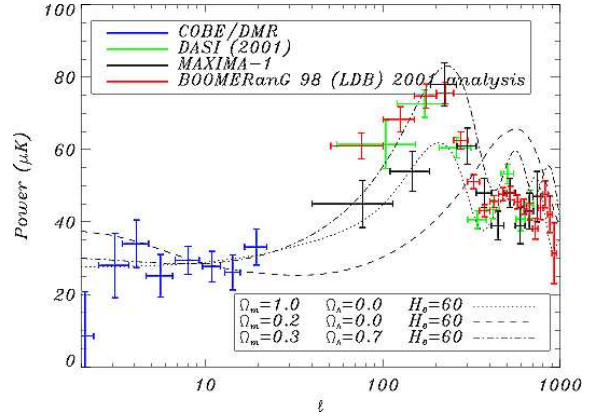


Figure 1. Expected CMB power spectrum  $\left(\sqrt{\frac{\ell(\ell+1)C_{\ell}}{2\pi}}\right)$  for inflationary-like primordial density fluctuations (black curves) for three different cosmological models along with the latest measurements from BOOMERanG, MAXIMA and DASI and the earlier measurements from COBE.

## 1.2. Recent results

Our knowledge of the CMB power spectrum has been significantly improved since COBE measurements [5] by two balloon-borne experiments, BOOMERanG [9] and MAXIMA [10], and a ground based interferometric experiment, DASI [12]. These results are shown in Figure 1. We observe that the very low part of the power spectrum is highly constrained by the COBE points while the high- $\ell$  acoustic region is constrained by the three recent experiments showing undoubtedly the multiple peak feature that is expected from inflation. This set of data therefore strongly disfavors topological defects as seeds for the structure formation in the Universe. Comparing this set of data with theoretical power spectra have lead to the estimation of the cosmological parameters [9,11,14]. The favored model is dominated by dark energy (around 70%) such as cosmological constant or quint essence (in agreement with high redshift type Ia supernovae measurements [15,16]). The 30% of matter consists

mainly of dark matter and the amount of baryons is in agreement with Big-Bang nucleosynthesis predictions and light elements abundances measurements. One of the great news coming from these results is that they agree very well with other measurements of the cosmological parameters obtained with completely different methods: large scale structure observation, lensing, type Ia supernovae and light elements abundances. We are now heading towards a concordance model.

### 1.3. Motivations for an intermediate scale experiment

There is a part of the CMB power spectrum that lacks measurements: between the large angular scales measurements from COBE (around  $\ell = 20$ ) and the largest angular scales from BOOMERanG, MAXIMA and DASI (above  $\ell \simeq 75$ ). This can be easily understood as when you are trying to measure large  $\ell$ , you concentrate on a small patch of the sky in order to reach high signal to noise ratio. This implies loosing all information on large scales. On the other hand, COBE covered the entire celestial sphere but with a poor 7 degrees resolution that limited the measurements to the low  $\ell$ . The intermediate part of the power spectrum, despite being difficult to measure, is of high interest: first, this is the part of the power spectrum that is the most sensitive to the early Universe physics. Second, linking COBE measurements to high- $\ell$  measurements with one single experiment would ensure that no calibration problems are affecting the data.

Archeops is a balloon-borne experiment designed to measure the CMB temperature angular power spectrum from the large multi-degree scales ( $\ell \simeq 30$ ) to the small sub-degree scales ( $\ell \simeq 800$ ). This is achieved via a large sky coverage (around 35%) along with a high angular resolution (10 arcminutes). Archeops is also very similar to Planck High Frequency Instrument and can therefore be considered as a real size testbed for Planck-HFI.

## 2. Archeops instrument

The Archeops instrumental setup<sup>2</sup> is exhaustively described in [17] and we will only outline its main characteristics.

### 2.1. Telescope and scanning strategy

The Archeops telescope is an off-axis Gregorian telescope with a 1.5 meter primary mirror that looks at 41 degrees of elevation. During the flight, the gondola rotates at 2 rounds per minute around its vertical axis and therefore performs scans on the sky at constant elevation. While the Earth rotates, these scans end up forming a wide annulus on the sky with scans crossing each other at various time scales allowing an efficient monitoring of systematic signals. The gondola is shown in Figure 2 and the scanning strategy in Figure 3. The gondola is hanged below a stratospheric balloon that floats at an altitude of around 40 km. The data is taken during 24 hours nighttime winter arctic flights.

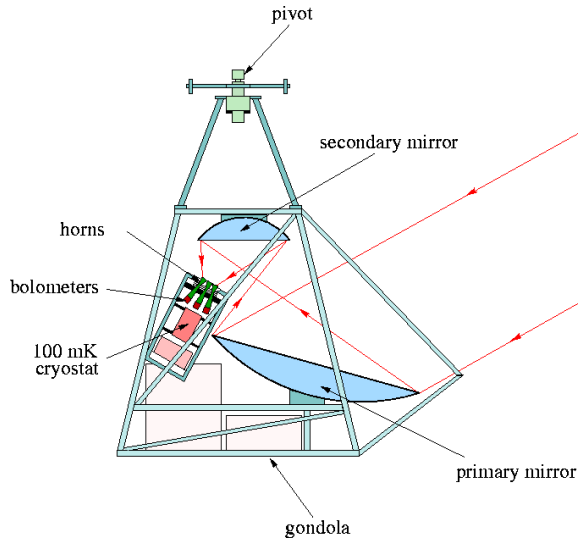


Figure 2. Schematic view of the Archeops gondola. The telescope observes at 41 degrees of elevation and rotates at 2 rounds per minute.

<sup>2</sup>see <http://www.archeops.org>.

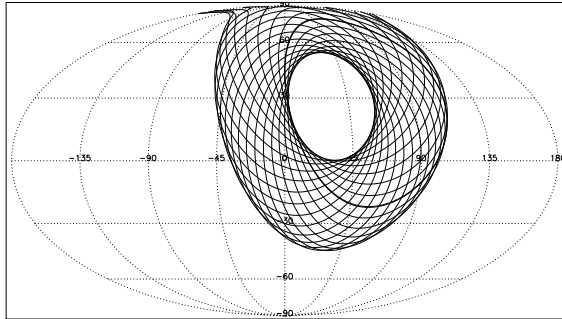


Figure 3. Scanning strategy on the sky (Molleweide projection): a circle is plotted every hour. After 24 hours, the covered region has the shape of an annulus.

## 2.2. Cryostat, bolometers and cold optics

The cryostat is a  $^3\text{He}$  –  $^4\text{He}$  dilution refrigerator that cools down to 100 mK. This dilution is the same that will be used for Planck-HFI and does not rely on gravity. The  $^3\text{He}$  –  $^4\text{He}$  mixing is made through capillaries all around the 100 mK stage. The radiation enters through a large (16 cm) polypropylene window closed by a valve that opens automatically at low pressure. The radiation is focused through Planck-HFI-like flared corrugated back-to-back horns at the 10 K stage. The lower part of the horns contains the filters in the 1.6 K stage. They filter 4 different frequencies depending on the bolometer: 143, 217, 353 and 545 GHz. The bolometers are located on the focal plane cooled down to 100 mK at the exit of flared horns. The bolometers are spider web bolometers similar to those that will be used for Planck-HFI [18]. Their nominal noise equivalent power (NEP) is  $1.4 \times 10^{-17}\text{W}/\sqrt{\text{Hz}}$ .

## 3. Archeops flights

The first Archeops test flight took place on July, 18<sup>th</sup> 1999 from the Italian balloon launching facility in Trapani (Sicily) to the South of Spain where the gondola landed on the next day. This test flight gave us 4 hours of good quality

night-time data with the 6 bolometers that were mounted in the focal plane. This flight helped us in improving the instrument in order to reduce systematic effects.

The first scientific flight took place in January, 29<sup>th</sup> 2001 from the SSC<sup>3</sup> base of Esrange (used by CNES<sup>4</sup>) in Kiruna in the North of Sweden. The focal plane contained 23 bolometers (one of them was blind in order to monitor systematic effects) with the following repartition: 8 bolometers at 143 GHz, 6 at 217 GHz, 6 at 353 GHz (sensitive to polarization using orthomode transducers) and 2 at 545 GHz. The interest in covering various frequencies is that we can monitor this way systematic effects and astrophysical foregrounds. During the flight, the temperature of the focal plane remained well below 100 mK (minimum of 89 mK) showing a perfect behavior of our cryostat. Unfortunately, due to unusually high stratospheric winds, we used a rather small balloon (150 000 m<sup>3</sup> instead of 400 000 m<sup>3</sup>) and the maximum altitude of the gondola was 31.5 km inducing a higher background and atmospheric contamination. Also due to these winds, the gondola arrived too fast to our Eastern limit (Ural mountains) and therefore we had to stop the flight after 7.5 hours at ceiling. This reduced considerably the amount of data taken during the flight and especially the highly redundant scans that start after 7 hours of flight. The quality of the data was however excellent and allows us to perform a CMB anisotropy analysis, especially on the low  $\ell$  edge of the first acoustic peak.

## 4. Data analysis

The data obtained in such an experiment consists of a set of time streams that represent the value of some detector (thermometer, bolometer, gyroscope, ...) as a function of time sampled at 153 Hz. The data analysis is performed through successive steps described in the following subsection.

<sup>3</sup>Swedish Space Corporation.

<sup>4</sup>Centre National d'Etudes Spatiales, the French space agency.

#### 4.1. Pointing reconstruction

During the flight, the gondola pendulates and does not rotate at constant speed, we therefore have to reconstruct off line the direction pointed by each bolometer for each sample. This is done using a stellar sensor telescope that is attached to the gondola and points in the same direction as the bolometers. The stellar sensor focal plane contains 48 photodiodes whose signal exhibits a peak whenever they cross a star. We therefore obtained an observed star catalog that is compared with a real one in order to give the pointing solution. Our pointing accuracy is estimated to be around one arcminute.

#### 4.2. Data cleaning

The data coming from the bolometers is characterized by long drifts that are correlated to the temperature variations inside the cryostat, pendulations and altitude variations. There is also a scan synchronous parasitic signal that can be monitored using high frequency channels. These extra signal are decorrelated and we are left with a time stream that still exhibits low frequency drifts due to imperfections in the decorrelation and residual signals.

#### 4.3. Beam reconstruction

During the scientific flight, Jupiter was observed twice with an interval of roughly two hours. We use Jupiter to obtain maps of our beams as its angular size (around 40 arcsec) is much smaller than our angular resolution. The beam maps for all off our bolometers are shown in Figure 4. We obtain an average angular resolution of around 12 arcminutes, larger than expected due to the large time response of the bolometers that can be seen in the figure on left side of each beam.

#### 4.4. Calibration

Jupiter can be used to calibrate our data as its surface brightness temperature is known to be  $170K_{RJ}$  with an uncertainty of 15%. This gives us a point source calibration. But the best calibration is obtained on extended sources like the Galactic plane and the cosmological dipole that both fill the beam, therefore including possible sidelobes. We obtained at the end a calibration

for each bolometer with an accuracy of 15%. The uncertainty is mainly due to the residual scan synchronous parasitic signal.

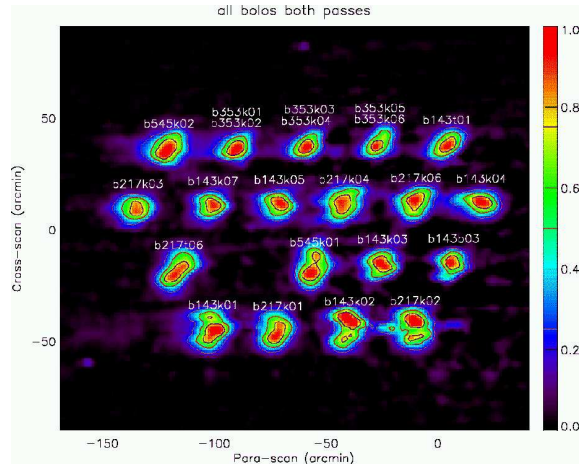


Figure 4. Measured beam shapes for the Archeops bolometers.

#### 4.5. Power spectrum estimation

We use the MASTER method [19] in order to measure the power spectrum on our maps. Within this framework, maps are obtained by coadding the filtered timelines on the sky. In the case of pure white noise, this leads to optimal maps. We filter our timelines keeping only frequencies between 1 and 45 Hz so that the resulting power spectrum is very close to be white. The pseudo- $C_\ell$  spectrum is obtained using *anafast* in Healpix package [20]. We then estimate the noise angular power spectrum on the coadded maps using a set of Monte-Carlo simulations. The effect of the filter on the underlying sky is also estimated via Monte-Carlo simulations. The mode mixing effect is deconvolved following [19]. All these corrections allow us to transform the pseudo- $C_\ell$  spectrum into a real angular power spectrum. We estimated the non optimality of our power spectrum (due to the non optimal maps) to be less than 30% at all scales.

The power spectrum estimation is at the moment under test. The expected accuracy for 10 bolometers, obtained through full simulations from timelines to power spectrum with realistic noise (measured on the real timelines), is shown in top panel of Figure 5.

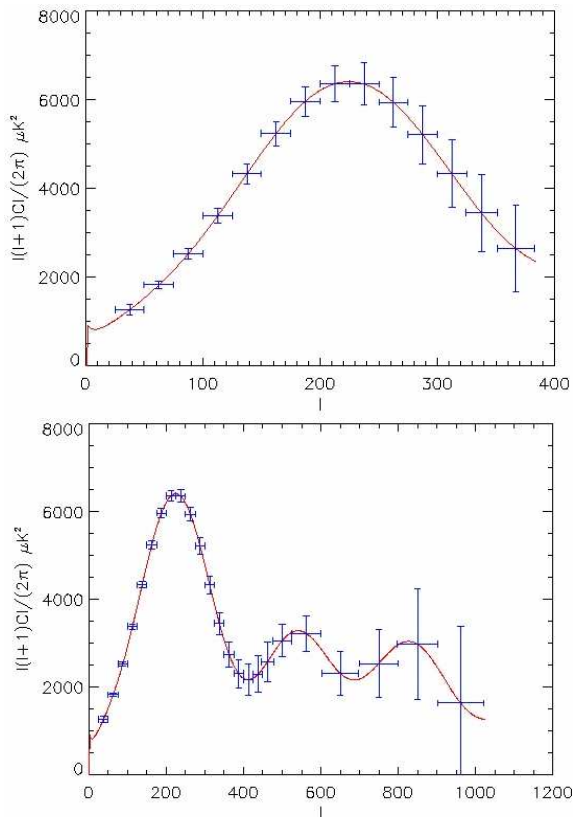


Figure 5. Estimated power spectrum accuracy for the 7h30 Kiruna scientific flight (top) and for the incoming 24 hours flights (bottom). Both were obtained for 10 bolometers from the average of one thousand realistic simulations of the Archeops timelines and noise structure.

## 5. Perspectives for incoming flights

A flight campaign is planned for Archeops this winter. We plan to flight once in December 2001 and once in January 2002. We will be able to achieve two 24 hours flights at high altitude (around 40 km). This will give us much more redundancies than on the previous 7h30 flight and cleaner data due to a higher altitude. The expected accuracy on the CMB angular power spectrum was estimated using the noise measured for the last flight, 10 bolometers, but for a 24 hours flight. The result is shown in the bottom panel of Figure 5.

These simulations show clearly that Archeops will be able to measure precisely the angular power spectrum of the CMB on both small and large angular scales. The improvement compared to previous experiment will be particularly significant on the low- $\ell$  part of the power spectrum (smaller error bars and better sampling).

## REFERENCES

1. A.A. Penzias and R.W. Wilson, *ApJ Lett.* **142**, 419 (1965).
2. R. Dicke *et al.*, *ApJ Lett.* **142**, 383 (1965).
3. G. Gamow, *Nature*, **162**, 680 (1948).
4. R. Alpher and R. Herman, *Nature*, **162**, 774 (1948).
5. G. Smoot *et al.*, *ApJ Lett.* **395**, L1 (1992).
6. J. Mather *et al.*, *ApJ* **420**, 439 (1994).
7. D. Fixsen *et al.*, *ApJ* **473**, 576 (1996).
8. U. Seljak and M. Zaldarriaga, *Proc. XVI<sup>th</sup> Moriond Meeting*, 241 (1997).
9. C.B. Netterfield *et al.*, [astro-ph/0104460](http://arxiv.org/abs/astro-ph/0104460).
10. S. Hanany *et al.*, *ApJ* **545**, L5 (2000).
11. A. Balbi *et al.*, *ApJ* **545**, L1 (2000).
12. N.W. Halverson *et al.*, [astro-ph/0104489](http://arxiv.org/abs/astro-ph/0104489).
13. C. Pryke *et al.*, [astro-ph/0104490](http://arxiv.org/abs/astro-ph/0104490).
14. D. Bond *et al.*, [astro-ph/0011378](http://arxiv.org/abs/astro-ph/0011378).
15. S. Perlmutter *et al.*, *ApJ* **483**, 565 (1997).
16. B.P. Schmidt *et al.*, *ApJ* **507**, 46 (1998).
17. A. Benoît *et al.*, [astro-ph/0106152](http://arxiv.org/abs/astro-ph/0106152).
18. P. Mauskopf *et al.*, *Appl. Opt.* **36** (1997).
19. E. Hivon *et al.*, [astro-ph/0105302](http://arxiv.org/abs/astro-ph/0105302).
20. K.M. Górski *et al.*, [astro-ph/9812350](http://arxiv.org/abs/astro-ph/9812350), <http://www.eso.org/kgorski/healpix/>